JOURNAL OF NANO AND MATERIALS SCIENCE RESEARCH
Volume 1 (Maiden edition, 2022), pp. 76-82
Available online at journals.nanotechunn.com/jnmsr

ORIGINAL ARTICLE

Microstructural and Corrosion Studies of Ni-P/Rice Husk Ash Composite Coatings on Mild Steel

F. U. Whyte[a,c,], A. L Mgboh[a], G. M. Whyte[b], and P. O. Offor[a,c]*

[a] *Department of Metallurgical and Materials Engineering, University of Nigeria Nsukka, 410001 Nsukka, Nigeria.*
[b] *Department of Physics and Astronomy, University of Nigeria Nsukka, 410001 Nsukka, Nigeria.*
[c] *Africa Centre of Excellence, ACE-SPED, University of Nigeria Nsukka, 410001 Nsukka, Nigeria*

KEYWORDS

Electroless plating,
Rice Husk Ash (RHA) particles,
Corrosion,
Composite Coating,
Microstructure

ARTICLE HISTORY

Received: Feb. 20, 2023
Revised: Feb. 24, 2023
Accepted: Feb. 27, 2023
Published: Feb. 27, 2023

ABSTRACT

This study investigated the effect of Rice Husk Ash (RHA) particles incorporation in electroless Ni-P coatings on the microstructural and corrosion properties of mild steel. In this study, pure Ni-P and Ni-P/RHA composite coatings were developed at different concentrations of rice husk ash particles (2g/l, 4 g/l, 6 g/l, and 8g/l) in an electroless bath. The effect of the RHA on the deposition rate, surface morphology and the corrosion properties of the coating was studied. The results show an increase in the deposition rate due to the inclusion of the RHA particles in the electroless plating bath indicating good bonding between the Ni-P matrix and the RHA particles. Further, the study of the surface morphology of the coatings using Scanning Electron Microscope (SEM) and Energy Dispersive Spectrometry (EDS) showed a sparse dispersion of the coating on the substrate and the SEM image of the Ni-P/8g RHA composite coating indicated that the rice husk ash was successfully incorporated in the electroless Ni-P coating as the SEM images had less voids and the EDS showed an increase in the deposition of Ni and P indicated by its higher percentages in the composite coating than in the pure Ni-P coating. Tafel polarization studies of the coating showed an increase in the corrosion rate of the coating with the addition of RHA particles. The Ni-P/4g RHA composite coating having the highest corrosion resistance of 16.94 mil/yr with an Ecorr of -0.301 V. This study confirms the effect of third phase particles addition on the microstructure and corrosion properties of electroless Ni-P and shows that RHA particles can be used as a cheaper and ecofriendly alternative to improve the microstructural and corrosion properties of electroless Ni-P coatings.

1 Introduction

Mild steel is applied in many areas such as structures, machine parts, oil fields, automotive industry, and many others [1]. However, mild steel has carbon content of about 0.05% to 0.25% [2]. It is known for its susceptibility to corrosion, as a result, several approaches have been taken to control its corrosion rate which includes coating, galvanization, and cathodic protection.

Coating materials is a good way to improve materials corrosion and wear resistance and coatings are of different types such as metallic coating which is a type of coating which comprises electroless coating, electroplating, among others [3].

Electroless coating, also known as auto-catalytic or chemical coating, is a non-galvanic coating method which involves several concurrent reactions in an aqueous solution and occurs without the supply of electrical power. It is different from electroplating because it does not require external electrical power [4]. Electroless coating involves continued deposition on the substrate because of the selective reduction of the metal ion from its aqueous solution on the catalytic substrate's surface through the catalytic action of the deposit itself [5].

* **CORRESPONDING AUTHOR** | F. U. Whyte | ✉ favour.otung@unn.edu.ng

Electroless nickel coating entails the reduction of nickel ions to nickel metal via chemical reduction. Here, Sodium hypophosphite is majorly used, others are sodium borohydride and dimethylamine borane, but they are not used frequently. It is found that sodium hypophosphite is used in more than 99% of all electroless nickel coating. It is undoubtedly the most important catalytic coating process in use today [6]. The electroless coatings is popularly used in aerospace, automobile, mechanical, and chemical industries due to its ability to produce friction resistant, wear resistant, hard and corrosion resistant surface nowadays [7].

As is well known, corrosion is a major drawback in mild steel usage especially in acidic environment. Thus, to improve the coating properties of the Ni–P deposits, second phase particles are added into the Ni–P matrix coatings consisting of hard particles, e.g., SiC, WC, Al_2O_3, Si_3N_4, TiO_2, ZrO_2, etc. [8].

Interestingly, research on the effect of incorporation of SiO_2 into Ni-P has been carried out and improved coating properties were recorded. Allahkaram S. R. and Rabizadeh T. [9] studied the effect of Ni-P/nano-SiO_2 electroless coatings on carbon steel. Their results showed improved microhardness due to the presence of the SiO_2 nanoparticles and the Ni-P/nano-SiO_2 gave the best corrosion resistance in comparison to the substrate and Ni-P. Similarly, Dong D. et al [10] observed an increase in hardness and wear resistance with incorporation of nano-SiO_2 into Ni-P with the composite coating heat treated at 400 ℃ having the maximum hardness and wear resistance.

Rice husk particles are agro-wastes and have been used by different researchers in various areas such as biomass fuel, brewing, adsorption materials. Rice husk ash is very high in silica. In this sense it has high hardness and wear resistance. Rice husk extract is an excellent corrosion inhibitor due to its ability to decrease corrosion rate of mild steel [11].

The research interest however is to investigate the effect of rice husk ash particle incorporation in electroless Ni-P coating on mild steel and determine its effect on the microstructural and corrosion resistance of the coating.

2 Materials and Methods

2.1 Surface Preparation of the Mild steel plate

The mild steel sheet was obtained locally and cut into dimension of (50×50×1) mm^3. The plates were ground with SiC papers of different sizes up to grit 1000 and they were ultrasonically cleaned in acetone for 5 mins after which it was immersed in ethanol, and acid pickling was done in 8% sulphuric acid for 1 minute. After each step, the specimens were rinsed in distilled water then immersed into the electroless bath.

2.2 Rice Husk Ash (RHA) Preparation and Characterization

The rice husk was obtained from Adani rice mill, Nsukka, Nigeria. It was washed thoroughly with water, dried in an oven at a temperature of 150 ℃ and ground in an electric grinding machine. Calcination of the dried rice husk was done in a heat treatment furnace for 4 hours at a temperature of 700 ℃ and sieved on a vibrating sieve machine with sieve of grit size 75 μm.

Fourier Transform Infra-red Spectra (FTIR) analysis was carried out on the rice husk ash using Buck scientific M530 USA FTIR equipment. This instrument was equipped with a detector of deuterated triglycine sulphate and beam splitter of potassium bromide. The software of the Gram A1 was used to obtain the spectra and to manipulate them. Approximately, 1.0 g of samples, 0.5 ml of Nujol was added, they were mixed properly and placed on a salt pellet. During measurement, FTIR spectra was obtained at frequency regions of 4000 – 600 cm^{-1} and co-added at 32 scans and at 4 cm^{-1} resolution. FTIR spectra were displayed as transmitter values.

2.3 Preparation of the Electroless Ni-P/Rice Husk Particle Plating Bath

The main compositions of the electroless bath are:

- Nickel sulphate salt ($NiSO_4$) for the nickel source
- Sodium hypophosphite (NaH_2PO_2) as reducing agent
- Lactic acid: complexing agent to complex nickel ions
- Propionic acid
- Lead acetate
- Fine rice husk ash of size 75 μm

The electroless coating process was basically done by dipping the substrate (mild steel) in a 1 litre of water solution containing different composition of the bath components [12]. Before the introduction into the bulk plating solution, the rice husk ash was stirred in a small part (about 200 ml) of plating solution by using magnetic stirrer to facilitate homogenous suspension of the particles and then poured into the bulk plating solution. The stirring speed was kept constant throughout the process for all the samples.

For the pH regulation, sodium hydroxide and sulphuric acid were used respectively. The composition contained in the plating bath is shown in Table 1. The plated samples were removed from the plating solution after one hour, rinsed in distilled water, cleaned, dried, and weighed.

Table 1: Chemical composition of electroless Nickel plating bath

Component	**Concentration (g/l) of Ni-P/RHA bath**
Nickel sulphate ($NiSO_4$)	21
Sodium hypophosphate ($NaPO_2H_2$)	24
Lactic acid	25
Propionic acid	3
Lead acetate	3 ppm
Rice Husk Ash	0, 2, 4, 6, 8
Operating Conditions	
pH	4.5 ± 0.2
Temperature	90 ℃ ± 2
Stirring speed	900 rpm

There were different amounts of rice husk ash particle added to each of the four different baths and a control bath in which no rice husk ash particle was added as shown in Table 2.

Table 2: Formulated design bath composition of Ni-P/rice husk ash composite coating

Sample Order	Matrix Sample	Time of Deposition (hours)	Rice Husk Ash (g)	Coating Temperature (℃)
0	Steel Substrate	1	-	-
1	Ni-P	1	-	90
2	Ni-P-2g RHA	1	2	90
3	Ni-P- 4g RHA	1	4	90
4	Ni-P- 6g RHA	1	6	90
5	Ni-P- 8g RHA	1	8	90

2.4 *Characterization*

The deposition rate (in μmh^{-1}) was calculated using eq. 1:

$$\frac{(W_2 - W_1) \times 1000}{(\rho \times A \times t)} \quad (1)$$

Weight of samples before and after plating are represented by W_1 and W_2 respectively, ρ represents the density of electroless coating (7.9 g/cm^3), A stands for a sample surface area (cm^2) and t shows the time of deposition (hr).

By using a digital scale, all samples' weights were recorded before and after the plating for 1 h [13]. Scanning Electron Microscopy/Energy Dispersive Spectrometry (SEM/EDS) was used to carry out microstructural analysis on the plated and unplated samples. The cut 10 × 10 mm sized samples were cold mounted using epoxy resin, gripped with the sample holder, and etched before being put in the sample chamber where the characterization was done. The SEM/EDS was done using the TESCAN SEM at an accelerating voltage of 20 KV. The corrosion analysis was done in 3.5 wt% NaCl solution (simulated sea water) at room temperature of 25 ℃. It was performed using Open Circuit Potential-Time (OCPT) technique for a period of 300 secs and Tafel polarization technique.

Electrochemical analysis was done using the corrosion tester model CH Instruments Electrochemical Analyzer with the CH603 Software. After electroless deposition, the plated samples were washed in distilled water, dried in air, and mounted in epoxy leaving an uninsulated surface area of 1 cm^2 as the working area.

For the Tafel polarization test, the samples, Ag/AgCl and Platinum made up the three conventional electrode cells, and they were used as working, reference and counter electrodes, respectively. The test was done with a scan rate of 0.01 V/s and between potentials of -1.5 V to 1.5 V.

3 Results and Analysis

3.1 *Composition of Mild Steel*

A spectrometric test was performed on the steel substrate at general steel mills, Asaba, Nigeria to determine the alloying elements present. Table 3 shows the chemical composition of the steel. The result shows the substrate is low carbon steel since the percentage of carbon present in the steel is 0.043%.

Table 3: Chemical composition of the mild steel

Element	C	Si	Mn	P	Ni	Al	B	As	Fe
Percent (%)	0.043	0.017	0.11	0.041	0.043	0.008	0.001	0.058	99.7

3.2 *Characterization of Rice Husk Ash Particle*

FTIR technique was used to identify the characteristic functional groups, which are instrumental in determination of functional groups and organic compounds inherent in the rice husk ash powder.

The FTIR spectra of the rice husk ash is shown in Fig. 1; the graph shows the presence of peaks of C-Cl, Si-O-Si, C=C, C-0, COO, C-N, C-H, N-H and -OH at stretching bands (733.274 cm^{-1} and 833.735 cm^{-1}), 1022.013 cm^{-1}, (1396.933 cm^{-1}, and 1597.425 cm^{-1}), 1785.371 cm^{-1}, 2040.512 cm^{-1}, (2182.662 cm^{-1} and 2275.685 cm^{-1}), 2457.864 cm^{-1}, (2725.354 cm^{-1} and 2876.716 cm^{-1}), 3435.980 cm^{-1}, (3007.258 cm^{-1}, 3312.540 cm^{-1}, 3549.344 cm^{-1} and 3913.442 cm^{-1}) respectively.

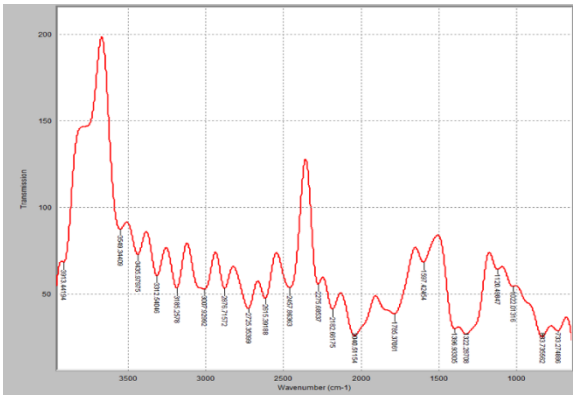

Fig. 1: FTIR spectra showing several bands for the rice husk ash (RHA) calcined at 700℃ for 4 hours

3.3 *Characterization of Coating*

The deposition rate of the coatings was determined from the weight increase of the sample after coating as shown in Table 4. Fig. 2 indicated a slight steady increase in the deposition rate of the sample with an increase in the amount of rice husk particles.

Kaleli et al [14] also observed bands due to presence of Silanol -OH and chemically absorbed water and Si-O-Si when he characterized rice husk ash prepared by open air burning and

furnace calcination at 700 ℃. The analysis indicates presence of Chloro-, Nitride-, Hydroxyl- and Silicon Oxide (SiO_2) compounds. The major constituent of the rice husk ash calcined at 700 ℃ for 4 hours was about 93% Silicon Oxide (SiO_2) [15].

Table 4: Corrosion parameters for all samples

Sample	R_p (KΩcm^2)	I_{corr} (μA/cm^2)	E_{corr} (V)	β_c (mV)	β_a (mV)	CR (mil/yr)
Steel substrate	0.056	958	-0.449	153.98	616.14	27.80
Ni-P	0.079	928	-0.441	139.43	248.14	21.69
Ni-P-RHA/2g	0.090	851	-0.402	123.57	630.52	18.78
Ni-P-RHA/4g	0.231	791	-0.301	103.58	365.63	16.94
Ni-P-RHA/6g	0.007	73	-0.517	173.67	320.92	418.60
Ni-P-RHA/8g	0.006	66	-0.531	132.80	347.71	315.90

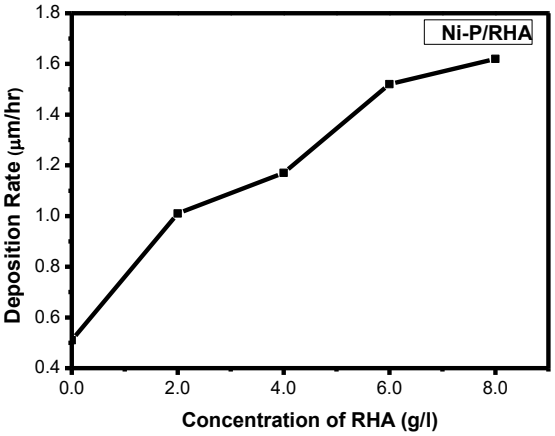

Fig. 2: Graph showing the effect of the concentration of rice husk ash (RHA) on the deposition rate

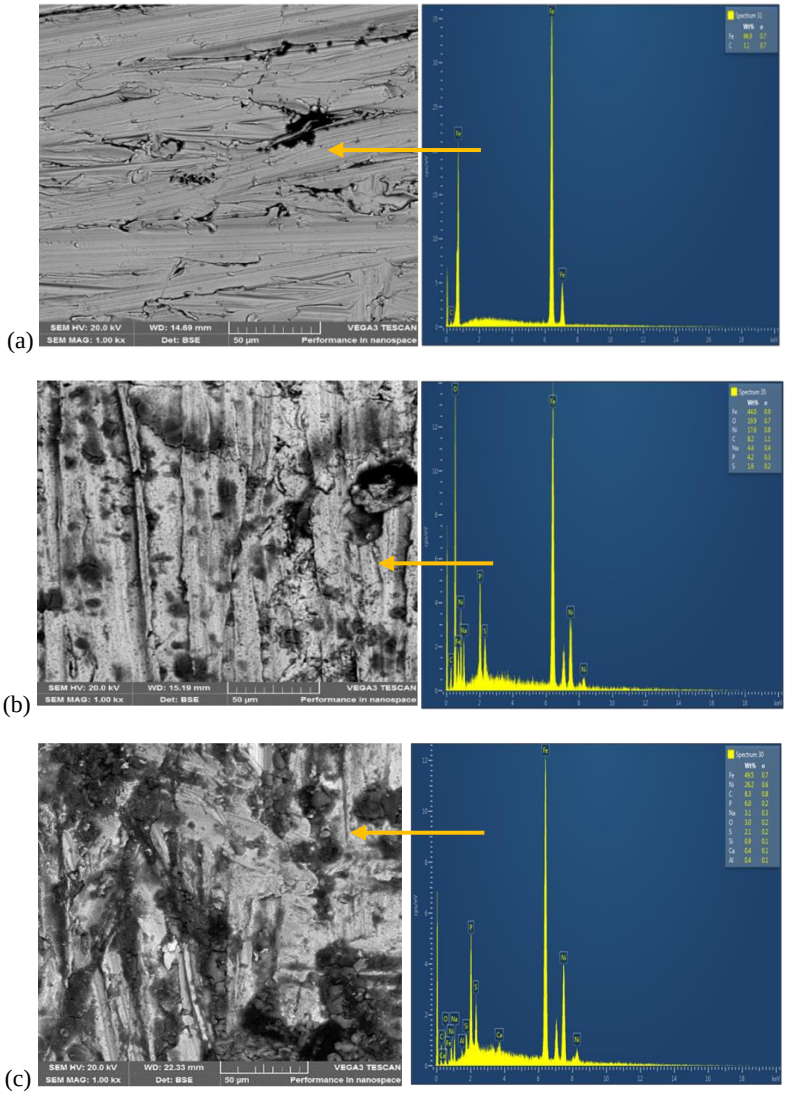

Fig. 3: SEM/EDS images (2000X) of a.) mild steel substrate b.) Ni-P c.) Ni-P/8g RHA

The increase in deposition rate indicates a good bonding of the rice husk particles with the Ni-P matrix with the Ni-P/8g RHA composite coating having the highest deposition rate of 1.62 µm/hr. This indicates that addition of the rice husk particles brought about grain filling and SiO_2 which was the major constituent of the rice husk ash improved the cementing properties of the coating. Generally, deposition rates were quite low, this might be due to the chosen bath parameters [16].

Scanning Electron Microscope (SEM) was used to observe the microstructural formations of the steel substrate, the electroless Ni-P and Ni-P/RHA coatings and Energy Dispersive Spectrometry (EDS) to determine the elements present and their percentages. SEM/EDS images of the mild steel substrate (Fig. 3a) showed fine needle like structures of Fe and C. The SEM/EDS of Ni-P showed sparse dispersions of the coatings and black spots which are micro pits or voids, common to Ni-P coatings of low thickness [17].

Fig. 3c showed a finer dispersion of the coatings with some cauliflower-like noodles and presence of less cracks or voids indicative of grain filling due to the good bonding of the RHA with the electroless Ni-P coating matrix. The cauliflower like noodles suggests the amorphous nature of the coatings. Also, the RHA inclusion improved the deposition of the Nickel and Phosphorous as the EDS indicated higher percentages of Ni and P values in the Ni-P/RHA composite coatings than in the Ni-P coatings.

The Corrosion studies of the substrate, pure and composite coated mild steel was carried out using the Open Circuit Potential – Time (OCPT) and the Tafel Polarization techniques. The open circuit potentials vs time, depicted in Fig. 4, shows the corrosion tendencies of the substrate and coatings when immersed in simulated sea water.

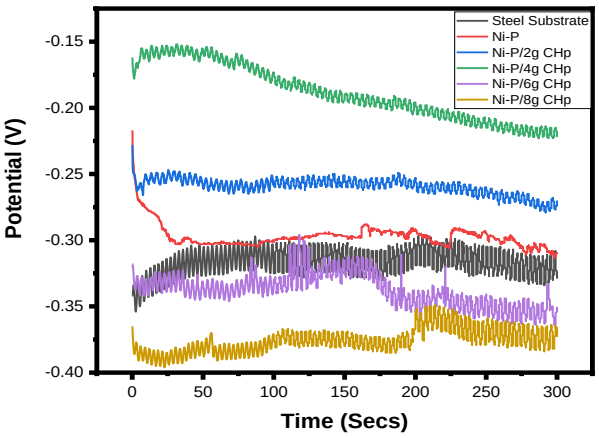

Fig. 4: Plots of Open Circuit Potential against immersion time for all samples

The substrate and the Ni-P/8g RHA composite coating had positive slopes which indicates their tendency to passivate while Ni-P and the Ni-P/2g-6g RHA composite coatings had negative slopes indicating its tendency to undergo general corrosion. The potential drop indicated by the negative slope shows formation of bare material while the increase in potential indicated by the positive slope shows passivation of the material which is indicative of better corrosion resistance as formation of oxides assists in slowing down the corrosion rate by forming a barrier [18] Generally, the coatings maintained a steady potential after a certain time, the times varied with the different coatings.

The plots for the Tafel polarization test done on all samples is shown in Fig. 5. The plots are like that observed by other researchers [19] and the graph shows that addition of RHA to electroless Ni-P brought about an increase in the corrosion potential until -0.301 V at 4g RHA addition after which a reduction in the corrosion potential was observed until the 8g RHA addition.

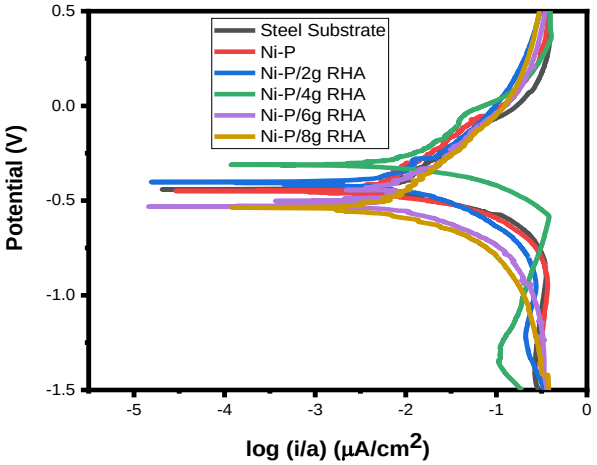

Fig. 5: Tafel plots for all samples

Increase in corrosion potential is due to the grain filling and reduction of voids observed in the SEM resulting from the addition of the RHA and since the addition of RHA increased deposition of Ni and P as observed by the EDS analysis (Fig. 3). Generally, the higher E_{corr}, lower I_{corr}, higher polarization resistance and higher corrosion resistance values of the composite coatings up to Ni-P/4g RHA as shown in Table 4 indicates that addition of RHA brought about an improvement in the corrosion resistance of the coatings. This is in line with the observation of Islam et al [20].

4 Conclusion

This study revealed that addition of rice husk ash has significant effects on the surface morphology and corrosion properties of the electroless Ni-P coatings. An increase in the deposition rate was observed with the Ni-P/8g RHA having the highest deposition rate of 1.62 μm/hr. Generally, the deposition rates were low which were due to the bath parameters used. Also, inclusion of rice husk ash particles in the electroless Ni-P bath brought about a slight modification in the microstructure of the composite coated mild steel with the composite coatings showing cauliflower-like noodles and less voids due to the RHA addition. Corrosion studies using the OCPT technique

revealed that some of the composite coated mild steels had the tendency to passivate and Tafel polarization tests indicated that addition of up to 4g RHA brought about an improvement in the corrosion resistance of the electroless Ni-P coatings. These results further confirmed that Ni-P/RHA composite coatings could be used for corrosion protection application in salty environments.

Acknowledgment

This research is sponsored by the TETFund Institution-Based Research (IBR) Intervention with research project No. TETFUND/DR&D/CE/UNI/NSUKKA/RP/VOL.1. The authors hereby acknowledge and appreciate the TETFund IBR, University of Nigeria Nsukka, Nigeria for the sponsorship.

Declaration of Competing Interest

Authors have declared that there is no existing conflict of interest.

References

[1] S. Ma, J. Xing, D. Yi, H. Fu, G. Liu, and S. Ma, "Microstructure and corrosion behavior of cast Fe–B alloys dipped into liquid zinc bath," Mater. Charact., vol. 61, no. 9, pp. 866–872, Sep. 2010, doi: 10.1016/j.matchar.2010.05.009.

[2] U. Anthony, M. Ikenna, O. B. Ufuma, and D. T. Ezemuo, "Corrosion Rates and its Impact on Mild Steel in Some Selected Environments," J. Sci. Eng. Res., vol. 3, no. 1, pp. 34–43, 2016, [Online]. Available: http://jsaer.com/download/vol-3-iss-1-2016/JSAER2016-03-01-34-43.pdf

[3] A. R. K. Abidali and A. M. H. Wais, "TRIBOLOGICAL BEHAVIOR OF Ni-P ELECTROLESS PLATING OF LOW ALLOY," Int. J. Mech. Prod. Eng. Res. Dev., vol. 9, no. 6, pp. 573–584, 2021.

[4] S. S. Djokic, Modern Aspects of electrochemistry, No. 48: Electrodeposition Theory and Practice. Springer Science+Business Media, LLC, 233 Spring Street, New York, NY 10013, USA, 2010.

[5] G. Mallory, "Electroless Plating : Fundamentals And Applications," Int. Bus., vol. 3, no. 2, pp. 103–111, 1990, Accessed: Aug. 20, 2022. [Online]. Available: https://books.google.com/books/about/Electroless_Plating.html?hl=de&id=2nmPKm6jEooC

[6] R. Parkinson, "Properties and applications of electroless nickel." https://nickelinstitute.org/~/Media/Files/TechnicalLiterature/PropertiesAndApplicationsOfElectrolessNickel_10081_.pdf (accessed Jan. 11, 2018).

[7] J. N. Balaraju, T. S. N. Sankara Narayanan, and S. K. Seshadri, "Electroless Ni-P composite coatings," J. Appl. Electrochem., vol. 33, pp. 807–816, 2003.

[8] A. Sharma and A. K. Singh, "Electroless Ni-P and Ni-P-Al2O3 nanocomposite coatings and their corrosion and wear resistance," J. Mater. Eng. Perform., vol. 22, no. 1, pp. 176–183, Jan. 2013, doi: 10.1007/S11665-012-0224-1.

[9] S. R. Allahkaram and T. Rabizadeh, "HIGH CORROSION RESISTANCE OF Ni - P /NANO- SiO 2 ELECTROLESS COMPOSITE COATINGS," Int. J. Mod. Phys. Conf. Ser., vol. 05, pp. 810–816, Jan. 2012, doi: 10.1142/S2010194512002784.

[10] D. Dong, X. H. Chen, W. T. Xiao, G. B. Yang, and P. Y. Zhang, "Preparation and properties of electroless Ni-P-SiO 2 composite coatings," Appl. Surf. Sci., vol. 255, no. 15, pp. 7051–7055, May 2009, doi: 10.1016/J.APSUSC.2009.03.039.

[11] M. Pramudita, S. Sukirno, and M. Nasikin, "Rice Husk Extracts Ability to Reduce the Corrosion Rate of Mild Steel," Int. J. Chem. Eng. Appl., vol. 9, no. 4, pp. 143–146, 2018, doi: 10.18178/ijcea.2018.9.4.715.

[12] P. Gadhari and P. Sahoo, "Effect of Annealing Temperature and Alumina Particles on Mechanical and Tribological Properties of Ni-P-Al2O3 Composite Coatings," Silicon, vol. 9, no. 5, pp. 761–774, Sep. 2017, doi: 10.1007/S12633-016-9452-6.

[13] R. Hu et al., "Deposition Process and Properties of Electroless Ni-P-Al2O3 Composite Coatings on Magnesium Alloy," Nanoscale Res. Lett., vol. 13, no. 1, p. 198, Dec. 2018, doi: 10.1186/s11671-018-2608-0.

[14] M. J. Kaleli, P. K. Kamweru, J. M. Gichumbi, and F. G. Ndiritu, "Characterization of rice husk ash prepared by open air burning and furnace calcination," J. Chem. Eng. Mater. Sci., vol. 11, no. 2, pp. 24–30, Oct. 2020, doi: 10.5897/JCEMS2020.0348.

[15] J. Shen, X. Liu, S. Zhu, H. Zhang, and J. Tan, "Effects of calcination parameters on the silica phase of original and leached rice husk ash," Mater. Lett., vol. 65, no. 8, pp. 1179–1183, Apr. 2011, doi: 10.1016/J.MATLET.2011.01.034.

[16] S. Afroukhteh, C. Dehghanian, and M. Emamy, "Preparation of electroless Ni-P composite coatings containing nano-scattered alumina in presence of polymeric surfactant," Prog. Nat. Sci. Mater. Int., vol. 22, pp. 318–325, 2012, doi: 10.1016/j.pnsc.2012.06.006.

[17] S. K. Tien, J. G. Duh, and Y. I. Chen, "The influence of thermal treatment on the microstructure and hardness in electroless Ni-P-W deposit," Thin Solid Films, vol. 469–470, no. SPEC. ISS., pp. 333–338, 2004, doi: 10.1016/j.tsf.2004.08.146.

[18] P. Ponthiaux, R. Bayon, F. Wenger, and J. P. Celis, "Testing protocol for the study of bio-tribocorrosion," in Bio-tribocorrosion in biomaterials and medical implants, 2013, pp. 372–394.

[19] F. G. Whyte, V. S. Aigbodion, G. M. Whyte, and I. C. Ezema, "Anti-corrosion and Wear Properties of Binary Ni–P/Cow Horn Particulate Composite Coatings on Mild Steel via Electroless Method," J. Bio- Tribo-Corrosion 2020 64, vol. 6, no. 4, pp. 1–8, Oct. 2020, doi: 10.1007/S40735-020-00431-1.

[20] M. Islam et al., "Influence of SiO2 nanoparticles on hardness and corrosion resistance of electroless Ni-P coatings," Surf. Coatings Technol., vol. 261, pp. 141–148, Jan. 2015, doi: 10.1016/J.SURFCOAT.2014.11.044.